ARTICLE

OBC
www.rsc.org/obc

Synthesis, characterization and coordination chemistry of the new tetraazamacrocycle 4,10-dimethyl-1,4,7,10-tetraazacyclododecane-1,7-bis(methanephosphonic acid monoethyl ester) dipotassium salt

Claudio Bianchini,[a] Giuliano Giambastiani,[a] Franco Laschi,[b] Palma Mariani,[c] Alberto Vacca,[c] Francesco Vizza *[a] and Piero Zanello [b]

[a] *Istituto di Chimica dei Composti Organometallici ICCOM-CNR, Via J. Nardi 39, 50132 Firenze, (Italy). E-mail: vizza@fi.cnr.it; Fax: +39 055 2478366; Tel: +39 055 245990*

[b] *Università di Siena, via Aldo Moro 1, Siena-53100, Italy*

[c] *Dipartimento di Chimica, Università di Firenze, via della Lastruccia 3, 50019 Sesto Fiorentino, Italy*

Received 29th October 2002, Accepted 9th January 2003
First published as an Advance Article on the web 12th February 2003

A new potentially hexadentate tetraazamacrocycle based on the *cyclen* skeleton has been synthesized and fully characterized. The macrocycle 4,10-dimethyl-1,4,7,10-tetraazacyclododecane-1,7-bis(methanephosphonic acid monoethyl ester) dipotassium salt ($Me_2DO2PME$) contains mutually *trans* monoethyl ester phosphonate acid substituents on two nitrogen atoms, and *trans* methyl substituents on the other two nitrogen atoms. The protonation constants of this macrocycle and the stability constants of its complexes with Cu^{2+}, Zn^{2+}, Gd^{3+} and Ca^{2+} ions have been determined by pH potentiometric titrations. The protonation sequence of the macrocycle has been studied by ^{1}H, $^{31}P\{^{1}H\}$ and $^{13}C\{^{1}H\}$ NMR spectroscopy: the first and second protonation steps take place at the methyl-substituted nitrogen atoms, while the third protonation involves one oxygen from a phosphonate group. Upon protonation, all the CH_2 ring protons become magnetically inequivalent on the NMR time scale due to a slow conformational rearrangement, most likely occasioned by the formation of multiple hydrogen bonds within the macrocyclic ring. Me_2DOPM forms neutral, mononuclear complexes with all the metals investigated. The presence of hydroxo complexes was observed for Ca^{2+} and Zn^{2+} at high pH values. Structural information on the neutral complex [Cu($Me_2DO2PME$)] has been obtained by a solution X-Band EPR study. It is proposed that $Me_2DO2PME$ binds Cu^{2+} in a distorted octahedral structure using all of its donor atoms, *i.e.* the four nitrogen atoms and the two phosphonate oxygen atoms. The redox chemistry of [Cu($Me_2DO2PME$)] in dimethyl sulfoxide and water has been studied by electrochemical measurements. Cyclic voltammetry in DMSO shows the complex to undergo a quasireversible one-electron reduction step leading to an unstable Cu^{I} species.

Introduction

Macrocyclic polyamines containing pendant arms with oxygen donor atoms are attracting considerable interest due to their ability to form complexes with a large variety of metal ions, spanning from transition metals to lanthanides. Such coordination compounds are generally featured by excellent thermodynamic stability, solubility in water and remarkable inertness to exchange metal ions *in vivo*.[1,2–4] For these reasons, polyazamacrocycle metal complexes are currently employed in resonance imaging (MRI),[5] biocatalysis as well as the synthesis of diagnostic and therapeutic radiopharmaceuticals.[6–8] Polyazamacrocycles with coordinating pendant arms are also being used as sequestering agents for toxic heavy metals such as mercury, lead and cadmiun.[9] A particular class of polyazamacrocycles is constituted by those bearing pendant phosphinic or phosphonic acid groups as they exhibit excellent coordination selectivity and high thermodynamic stability.[10] Indeed, the protonation of either phosphinate or phosphonate oxygen atom is difficult to accomplish in both the free ligand and metal complexes.[11] As a result, the metal complexes with phosphonate and phosphinate-substituted polyazamacrocycles are rather stable to proton-catalysed dissociation pathways, which is required for applications as labelled devices in therapy and *in vivo* imaging. Furthermore, structural variations of the phosphorus substituents may effectively control the hydro-lipophilic properties of both ligand and metal complexes, which may ultimately provide a fine tuning of the conjugation with proteins and other biologically active molecules.[12]

We have recently studied the ligand Me_2DO2A (1,7-dimethyl-1,4,7,10-tetraazacyclododecane-4,10-diacetic acid) and its ^{64}Cu-labelled complex. *In vivo* pharmacokinetic studies, carried out by Positron Emission Tomography, showed that the radiolabelled complex was able to cross the blood-brain barrier.[13] Intrigued by this result and by the possibility of tailoring the chemical and biological properties of similar metal complexes, we decided to design other polyazamacrocyclic ligands differing in either hydro-lipophilicity or overall charge of the resultant metal complexes.

In this work, we report the synthesis and characterization of the new *N*-functionalized tetraazamacrocycle 4,10-dimethyl-1,4,7,10-tetraazacyclododecane-1,7-bis(methanephosphonic acid monoethyl ester) dipotassium salt ($Me_2DO2PME$).

The protonation constants of this new macrocycle and the stability constants of its complexes with Cu^{2+}, Zn^{2+}, Gd^{3+} and Ca^{2+} ions have been obtained from pH potentiometric titrations, while the protonation sequence of the macrocycle has been determined by ^{1}H, $^{31}P\{^{1}H\}$ and $^{13}C\{^{1}H\}$ NMR spectroscopy. The solution structure of the complex [Cu($Me_2DO2PME$)] has been studied by X-band EPR spectroscopy.

Results and discussion

Synthesis and characterization of the macrocycle $Me_2DO2PME$ (L)

The ligand $Me_2DO2PME$ (**LK_2**) was obtained *via* the two-step sequence illustrated in Scheme 1.

In brief, the reaction of 4,10-dimethyl-1,4,7,10-tetraazacyclododecane with paraformaldehyde and diethyl phosphite in

DOI: 10.1039/b210655h

Table 1 Comparison of the stepwise protonation constants of $Me_2DO2PME$ with those of other macrocycle ligands (T = 298 K)

Ligand	logK_1	logK_2	logK_3	logK_4	Conditions
$Me_2DO2PME$[a]	10.63(1)	9.00(2)	1.89(6)		0.1 M NMe_4Cl
Me_2DO2A[b]	11.38(1)	10.38(1)	3.90(1)	2.30(1)	0.15 M NMe_4Cl
DO2PME[c]	11.14(0.015)	8.94			0.1 M KCl

Values in parentheses are standard deviations in the last significant figure. [a] This work; [b] Ref. 13; [c] Ref. 14.

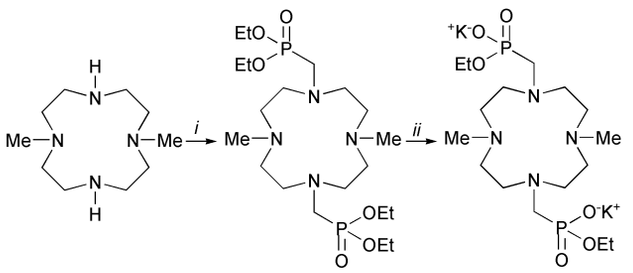

Scheme 1 Synthesis of $Me_2DO2PME$. i) diethylphosphite–$(CH_2O)_n$ ii) KOH.

dry toluene gave 4,10-dimethyl-1,4,7,10-tetraazacyclododecan-1,7-bis(methanephosphonic acid diethyl ester) in excellent yield. The following hydrolysis with KOH (3 M) at 100 °C for 2 h gave $Me_2DO2PME$ (4,10-dimethyl-1,4,7,10-tetraazacyclododecan-1,7-bis(methanephosphonic acid monoethyl ester) dipotassium salt in 77% yield as an off-white microcrystalline water-soluble solid.

The refined protonation constants of $Me_2DO2PME$ were determined by standard potentiometric titration methods. The data obtained are reported in Table 1 that also contains corresponding values for Me_2DO2A (1,7-dimethyl-1,4,7,10-tetraazacyclododecane-4,10-diacetic acid)[13] and DO2PME (1,4,7,10-tetraazacyclododecane 1,7-bis(methanephosphonic acid monoethyl ester)).[14] The values log K_1 = 10.63 (1), log K_2 = 9.00(2), and log K_3 = 1.89 (6), refer to the equations $Me_2DO2PME^{2-} + H^+ \leftrightarrows HMe_2DO2PME^-$, $HMe_2DO2PME^- + H^+ \leftrightarrows H_2Me_2DO2PME$ and $H_2Me_2DO2PME + H^+ \leftrightarrows H_3Me_2DO2PME^+$, respectively. A reliable value for the fourth protonation constants could not be determined due to its extremely low value.

The distribution of the species deriving from the protonation equilibria of $Me_2DO2PME$ is shown in Fig. 1.

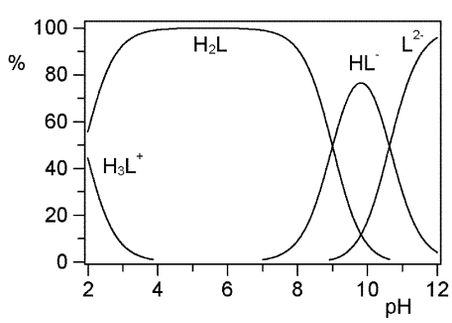

Fig. 1 Speciation diagram of $Me_2DO2PME$ protonation (298 K, I = 0.1 mol dm^{-3} NMe_4Cl). Species percentages are relative to total ligand.

Since the macroscopic protonation constants measured by potentiometry do not provide detailed information about the microscopic protonation sequence of the macrocycle, we decided to perform a ^1H, $^{13}C\{^1H\}$ and $^{31}P\{^1H\}$ NMR titration analysis in the pH range from 14 to 1. A sketch of the macrocycle with the labelling scheme adopted in the NMR analysis is shown in Fig. 2.

In order to interpret the variations of the chemical shifts as a function of the pH, it is assumed that the protonation of the methyl-substituted nitrogen atoms affects primarily the chemical shifts of the NCH_3 (A) protons, while the protonation

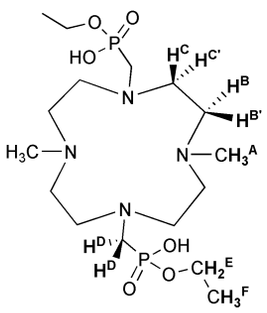

Fig. 2 Sketch of the macrocycle with the labelling scheme used.

of both the other two nitrogen atoms and the $P(O)(OEt)O^-$ group predominantly influences the chemical shifts of the NCH_2O (D) protons.

Irrespective of the pH, the A-type protons appear as a sharp singlet, while the protons of the D-type protons appear as a doublet (with $^2J_{HP}$ = 10.8 Hz). A plot of the chemical shift for protons A and D as a function of the pH at 25 °C is shown in Fig. 3. The strong inflection observed between pH 13.7 and 8 corresponds to the first and the second protonation in keeping with the potentiometric data listed in Table 1, and apparently involves protons A rather than protons D. These data indicate that on decreasing the pH from 13.75 to 8, a selective protonation occurs at both methyl-substituted nitrogen atoms. The second weak inflection appear below pH 2 and is attributed to small shifts of the D-type protons in consequence of the protonation of the phosphonate group. The variation of the chemical shifts of the phosphonate phosphorus atoms as a function of the pH is shown in Fig. 4. The downfield shift of δ_P in the pH region from 14 to 9 indicates that the first two protonations take place at the nitrogen atoms of the macrocycle and not at the phosphonate oxygen atoms.

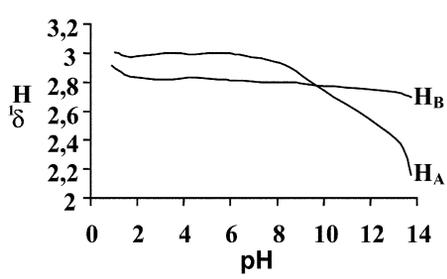

Fig. 3 ^1H NMR chemical shifts of H_A and H_D protons of $Me_2DO2PME$ *versus* pH measured at 200 MHz and 25 °C.

This behaviour is shared by all the known *N*-substituted phosphonic systems studied by NMR methods.[15] Consistent with the protonation of a phosphonic acid ethyl ester group, an upfield δ_P shift was observed in the pH region from 1 to 4.5, where the third protonation occurs. Analogous upfield shifts in the ^{31}P NMR titration curves have been reported for the protonation of phosphinic acids.[16]

In conclusion, the NMR study allows us to assign the first two protonation constants (log K_1 = 10.63 (1), log K_2 = 9.00(2)) to the protonation of the methyl-substituted nitrogen atoms, while the third protonation with log K_3 = 1.89 (6) involves a $P(O)(OEt)O^-$ group. It is worth noting that the first two

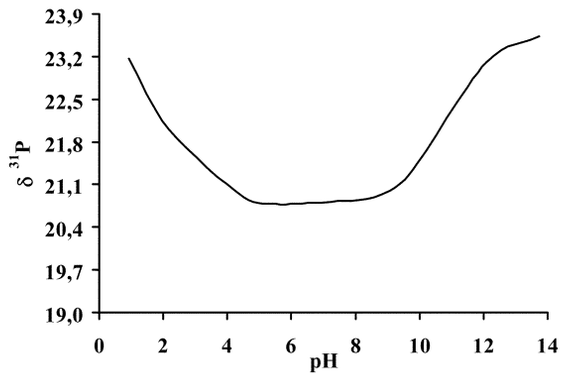

Fig. 4 $^{31}P\{^{1}H\}$ NMR chemical shifts of phosphorus atom of $Me_2DO2PME$ *versus* pH measured at 200 MHz and 25 °C.

protonation constants are smaller than those observed for Me_2DO2A as a reasonable consequence of the lower basicity of the macrocycle phosphonate $Me_2DO2PME$ in comparison to the carboxylate ligand Me_2DO2A. The very small value of the third constant is accounted for by the low basicity of $P(O)(OEt)O^-$ moiety. The first protonation constant is smaller than DO2PME according to the reduced basicity of tertiary ammines in water than secondary ammines.

A $^{13}C\text{-}\{^{1}H\}$ NMR study at different pH values was carried out in order to support further on the protonation sequence in the free ligand. Decreasing the pH from 13.75 to 1 did not significantly affect the ^{13}C-chemical shifts.

In agreement with the ^{1}H NMR analysis, the ligand is in the fully deprotonated form at high pH value (13.75). In such conditions, the CH_2 ring ^{1}H NMR resonances appear as a broad signal, while the signal of the H_D protons shows up as a doublet, which is consistent with a rapid inversion of the macrocycle ring. On decreasing the pH to 1, the CH_2 resonances split into four equally intense multiplets one of which partially overlapped with other signals (Fig. 5, trace a). The protons of the CH_2 bridging units are apparently diastereotopic with two geminal couplings of 14.0 ($^3J_{BB'}$) and 15.4 ($^3J_{CC'}$) Hz and four vicinal couplings of 3.4 ($^3J_{BC}$), 7.5 ($^3J_{BC'}$), 3.2 ($^3J_{B'C}$) and 3.0 ($^3J_{B'C'}$) Hz. The stereochemistry of the macrocycle in the pH range from 1 to 1.5, corresponding to the $\mathbf{H_3L}$+ species (Fig. 1), can be attributed to the formation of a network of multiple hydrogen bonds within the macrocycle. A similar pattern at low pH values has been reported for the internal CH_2 protons of Me_2DO2A.[13] Unambiguous assignment of the ^{1}H, and $^{13}C\text{-}\{^{1}H\}$ resonance at pH 1 was obtained from 2-D ^{1}H-COSY, $^{1}H\text{-}^{13}C$-HMQC and $^{1}H\text{-}\{^{31}P\}$ NMR spectra. Variable-temperature ^{1}H NMR experiments showed that the $\mathbf{H_3L^+}$ species has a rigid conformation even at 90 °C (Fig. 5, trace b).

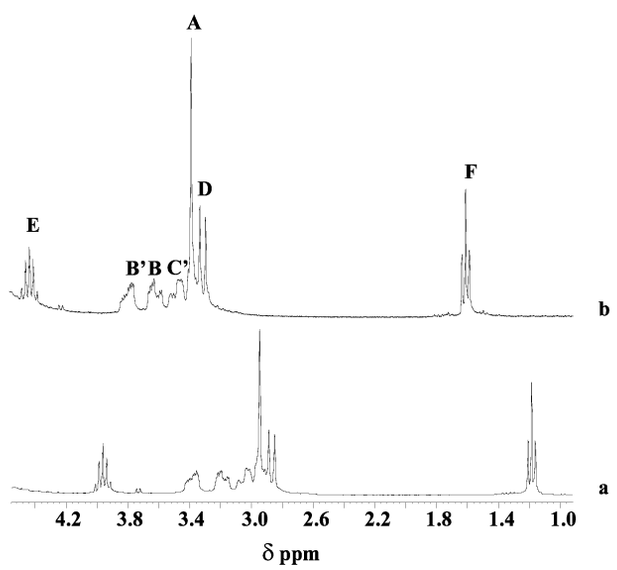

Fig. 5 ^{1}H NMR spectra of $Me_2DO2PME$ at pH 1: (a) at 25 °C; (b) at 90 °C.

Synthesis and characterization of [Cu(Me$_2$DO2PME)]

The reaction of $Me_2DO2PME$ with $Cu(ClO_4)_2 \cdot 3H_2O$ in MeOH gave the blue, mononuclear Cu^{II} complex $[Cu(Me_2DO2PME)] \cdot 3H_2O$ (**CuL**) featured by a μ_{eff} of 2.08 BM. This complex is extremely hygroscopic and all our attempts to obtain crystals suitable for an X-ray analysis were unsuccessful. The stability in water was determined by potentiometric measurements. As shown in Fig. 6, the only observed species was the mononuclear complex **CuL**, while neither the protonated form nor the hydroxylate form was observed at any pH between 2.5 and 7. The thermodynamic stability constant of **CuL** was found to be four log K units smaller than that reported for the corresponding $[Cu(Me_2DO2A)]$ complex.[13] The lower stability of **CuL** may be related to the lower basicity of the monoester phosphonate derivative as compared to the corresponding carboxylate macrocycle Me_2DO2A.

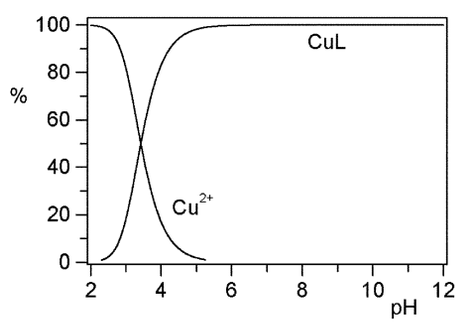

Fig. 6 Speciation diagram for the system Cu^{2+}–$Me_2DO2PME$ system (298 K, $I = 0.1$ mol dm^{-3} NMe_4Cl, metal to ligand ratio 1:1, $C_M = 0.001$ mol dm^{-3}). Species percentages are relative to total metal.

An EPR study of **CuL** was carried out in an attempt at determining its solution structure. Fig. 7a shows the liquid nitrogen (LN, T = 104 K) X-band EPR spectrum of the powder complex.

The spectrum line-shape is typical of an $S = 1/2$ metal system experiencing an extensive solid-state spin–spin interaction. The spectrum exhibits a broad and very poorly resolved axial structure (even in second derivative mode) with $g_{||} \geq g\perp \neq g_{electron} = 2.0023$. Due to the actual anisotropic line-width, neither the cupric hyperfine splittings (^{63}Cu: $I = 3/2$; natural abundance = 69.1%. ^{65}Cu: $I = 3/2$; natural abundance = 30.9%) nor the nitrogen superhyperfine splittings (^{14}N: $I = 1$, natural abundance = 99.6%) were observed. The ΔH_{av}(LN) line-width and the corresponding $g_{averaged}$(LN) parameter are 90(8) G and 2.107(5), respectively (Table 2). The powder spectrum at room temperature is similar to the LN spectrum, apart from minor variations of the Cu^{II} paramagnetic features (spectral intensity, $\Delta H_{anisotropic}$, $g_{anisotropic}$) due to active temperature-dependent Electron Spin relaxation mechanisms.[17]

Traces b (first derivative) and c (second derivative) in Fig. 7 show the LN X-band EPR spectra of **CuL** in methanol, while trace d illustrates the spectrum at room temperature. The glassy solution spectrum exhibits an axial structure with the perpendicular region partially overlapped to the parallel region in the intermediate field (traces b, c). The parallel region exhibits four well separated cupric hyperfine bands, while the perpendicular bands are overlapping each other giving a single broad line. An upper limit for the perpendicular hyperfine (hpf) cupric splittings may be estimated as $\Delta H_{||} \geq a(Cu)_{||}$. Computer simulation procedures allowed us to define the best fit EPR parameters, which are collected in Table 2.[18] No anisotropic nitrogen superhyperfine splitting was detected as a consequence of the actual line-width, largely overlapping the underlying

Table 2 Temperature dependent X-band EPR parameters of the solid state, CH_2Cl_2 and CH_3OH solutions of the CuL complex

$g_{\|}$	$g\perp$	$<g>$	$g_{isotropic}$	$A_{\|}$*	$A\perp$*	$<A>$*	$A_{isotropic}$*
		2.107(5)[a]		≤ $\Delta H_{\|}$§	≤ $\Delta H\perp$§		≤ $\Delta H_{isotropic}$§
		2.102(5)[b]		≤ $\Delta H_{\|}$§	≤ $\Delta H_{\|}$§		≤ $\Delta H_{isotropic}$§
2.196(5)[c]	2.060(5)[c]	2.106(5)[c]	2.107(3)[c]	12.4(5)[c] ≤ $\Delta H_{\|}$§[,d]	2.9(5)[c] ≤ $\Delta H\perp$§[,d]	6.1(5)[c]	7.5(3)[c] ≤ $\Delta H_{isotropic}$§[,d]
2.187(6)[e]	2.061(6)[e]	2.103(6)[e]	2.109(5)[e]	19.4(6)[e] ≤ $\Delta H_{\|}$§[,d]	≤5.2(6)[e] ≤ $\Delta H\perp$§[,d]		7.3(6)[e] ≤ $\Delta H_{isotropic}$§[,d]

$<g> = 1/3(g_{\|} + 2g\perp)$; $<a> = 1/3(a_{\|} + 2a\perp)$. *: A_i as $1 \times 10^{-3}cm^{-1}$. §: ΔH_i in Gauss. [a] solid state, T = 298 K; [b] solid state, T = 104 K; [c] MeOH solution; [d] A_i(N) shpf coupling; [e] CH_2Cl_2 solution

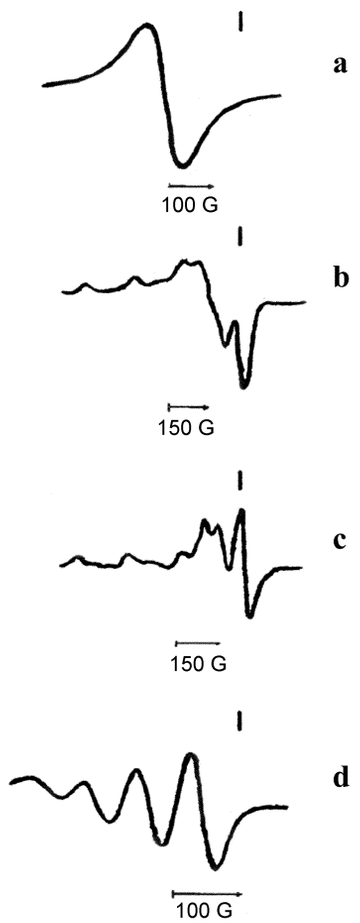

Fig. 7 X-Band EPR spectra of the solid state and CH_3OH solutions of the complex CuL (a) solid state at 104 K (LN); (b), (c) CH_3OH at 104 K (LN); (d) CH_3OH (RT).

a_i(N) splittings. Accordingly, the upper limits for both the perpendicular and parallel shpf splittings may be estimated as $\Delta H_{\|,\perp} > a(N)_{\|,\perp}$. On the basis of the Peisach–Blumberg approach, the tetrahedral distortion parameter $f = g_{\|}/a_{\|}$ suggests a N_2O_2 donor atom set for the xy equatorial coordination sites, leaving the z apical positions available for the two remaining nitrogen atoms in a distorted octahedral geometry.[13,19] At the glassy-fluid solution transition phase, the axial spectrum collapses into an isotropic spectrum (trace d). The fluid solution lineshape is well resolved in the four cupric hpf bands affected by significant line-width and magnetic field dependence on m_I(Cu) and $a_{isotropic}$(Cu), respectively. This spectral behaviour has been previously observed and attributed to structural anisotropies, not completely averaged in fast motion conditions.[13,17] No isotropic shpf resolution of the equatorially bound nitrogen atoms was seen; accordingly, taking into account the narrowest cupric $m_I = +3/2$ signal, an upper limit for such an interaction can be estimated as $\Delta H_{isotropic}(m_I = +3/2) \geq a_{isotropic}(m_I = +3/2)$. The isotropic parameters are reported in Table 2.

The relevant glassy $<g_i,A_i>$ values well fit the corresponding isotropic ones, suggesting that, under very different experimental conditions, the cupric complex maintains the proposed O_h geometry. In aqueous solution at room temperature, **CuL** displays a spectrum essentially identical to that in MeOH ($g_{isotropic}$ = 2.103(8); $A_{isotropic}$(Cu) = 7.7(8) × 10^{-3} cm^{-1}), while the frozen spectrum (T = 100 K) is poorly informative due to the very broad axial line-width. In these conditions, the parallel region is not visible, and the perpendicular region exhibits a unique broad and unresolved signal ($\Delta H\perp$ = 140(8)G, $g\perp$ = 2.087(6)).

In Table 2 are also reported the X-band EPR parameters of the copper(II) complex dissolved in CH_2Cl_2 solution at different temperatures. The temperature dependence of the line-shape and the relevant g_i parameters are significantly similar to those in MeOH, suggesting that the solvents investigated do not affect the primary geometry of the complex. It is worth noting, however, that the LN A_i cupric constants in CH_2Cl_2 are significantly higher than those observed in either MeOH or H_2O. This spectral behaviour suggests that the extent of the magnetic interaction between the unpaired electron and the copper nucleus is affected by the nature of the solvent (dielectric constant, molecular polarity). Apparently, the less polar solvent (CH_2Cl_2) favours the cupric hpf interactions.

The line-shape analysis suggests that the overall SOMO is mainly constituted by the copper(II) $3d_x^2-y^2$ orbital, with a very minor contribution arising from the AO's of the magnetically equivalent nitrogen and oxygen atoms in the equatorial plane.[13] The EPR parameters therefore highlight the importance of the Cu^{II} spin-orbit coupling constant ($\lambda < 0$) in determining the overall paramagnetic features of the complex.

The redox behaviour of **CuL** in solution was evaluated by electrochemical measurements. Fig. 8a shows the cyclic voltammograms of the complex in DMSO solution. The blank DMSO solution is electrochemically inactive in the range from +0.8 V to −2.1 V; a first cathodic process, exhibiting features of chemical reversibility, is followed by a second irreversible reduction, then by a further irreversible reduction. Controlled potential coulometry in correspondence to the first

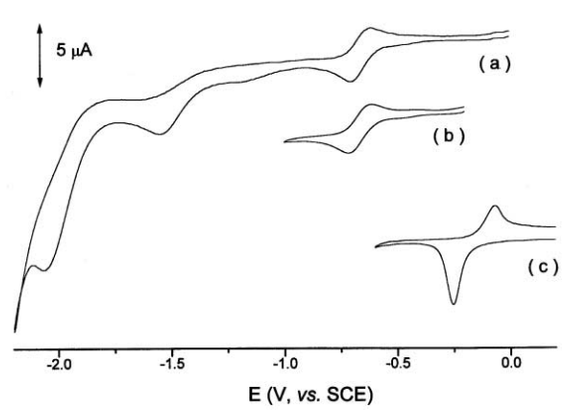

Fig. 8 (a, b) Cyclic voltammetric profiles recorded at a platinum electrode on a DMSO solution containing CuL (1.1 mol dm^{-3}). $[NBu_4][ClO_4]$ (0.1 mol dm^{-3}) supporting electrolyte. Scan rate 0.05 Vs^{-1}. (c) Cyclic voltammogram recorded at a platinum electrode on a aqueous solution containing [Cu(Me_2DO2PME)] (1.5 mol dm^{-3}). Phosphate buffer (pH 7.2) – NaCl 0.2 mol dm^{-3}). Scan rate 0.2 Vs^{-1}.

Table 3 Stability constants of the complexes formed by $Me_2DO2PME$ at 298 K, $I = 0.1$ M NMe_4Cl

Reaction [a]	log K^b Ca^{2+}	Cu^{2+}	Zn^{2+}	Gd^{3+}
M + L⟶ML	3.45(9)	16.10(2)	14.12(2)	9.75(1)
ML + OH⟶M(OH)L	3.6(2)		3.66(5)	
ML + 2OH⟶$M(OH)_2L$	7.2(2)		6.7(1)	

[a] Electrical charges are omitted for simplicity. [b] Values in parentheses are standard deviations on the last significant figure.

reduction ($E_w = -0.8$ V) was found to consume one-electron *per* molecule. Cyclic voltammetric tests on the resulting solution showed the almost complete disappearance of the relative peak-system, suggesting that the one-electron addition gives an unstable species. The cyclic voltammogram of the first cathodic process was analysed varying the scan rate from 0.02 to 1.00 V s^{-1}. This study showed that: i) the peak–current ratio i_{pa}/i_{pc} is lower than unity also at low scan rate (typically, at 0.05 V s^{-1} the peak–current ratio is 0.8) and does not increase appreciably with the scan rate; ii) the peak-to-peak separation is significantly higher than the theoretical value of 60 mV expected for an electrochemically reversible one-electron process (the observed separation was 100 mV at 0.02 V s^{-1} and progressively increased to 180 mV at 1.0 V s^{-1}); iii) the current function $i_{pc} \cdot v^{-1/2}$ is substantially constant. All these observables are diagnostic for a diffusion controlled, electrochemically quasi-reversible Cu^{II}/Cu^{I} reduction featuring partial chemical reversibility. In particular, the electrochemical quasi-reversibility suggests that the macrocycle cavity is not sufficiently flexible to support the increase of the atomic radius following the Cu^{II}/Cu^{I} reduction.

On the basis of the electrochemical study described above, it is reasonable to conclude that the first cathodic process ($E^{\circ\prime} = -0.66$ V, *vs.* SCE) is due to a Cu^{II}/Cu^{I} reduction leading to $[Cu(Me_2DO2PME)]^-$. The subsequent cathodic process ($E_p = -1.55$ V) is tentatively assigned to a Cu^{I}/Cu^{0} step, while the further multielectron process at $E_p = -2.06$ V is likely due to a ligand-centred electron transfer.

CuL undergoes severe poisoning in aqueous solution at both platinum and glassy carbon electrode. Therefore, any accurate electrochemical investigation was precluded. However, assuming the occurrence of a quasi-reversible one-electron step, an $E^{\circ\prime}$ value of -0.17 V may be calculated for the first cathodic process illustrated in Fig. 8c.

Stability constants of ML complexes (M = Ca^{2+}, Cu^{2+}, Zn^{2+}, Gd^{3+})

The stability constants of **CuL** as well as other complexes with Ca^{2+}, $Zn^{2+}$and Gd^{3+} were determined using potentiometric titrations of the macrocycle in the presence of each of these metal ions. The total ligand concentration was about 7×10^{-4} mol dm^{-3} in all measurements, while the metal ion concentration was in the range 2×10^{-4}–9×10^{-4} mol dm^{-3} for Ca^{2+}, Cu^{2+} and Zn^{2+} with pH values ranging from 2.5 to 10.5 for $Ca^{2+}$and Zn^{2+} and from 2.5 to 7 for Cu^{2+}. For the Gd^{3+} complex this procedure was impractical due to its extremely slow equilibration at lower pH values. For this reason, the "out of cell" technique was used. Ten different samples were prepared at different pH values between 2.5 and 6 and were allowed to equilibrate during four weeks. After the equilibration was reached at each experimental pH values, final readings were taken and used to evaluate the stability constants. As shown in Table 3, the ligand forms only 1:1 complexes with all the metals studied. In agreement with the strong acidity of the phosphonic acid ester group $PO(OEt)O^-$, the formation of the protonated complexes was not observed. This finding is actually in line with the relatively low stability constants of these complexes as compared to those formed by DOTA (1,4,7,10-tetraazacyclododecane-1,4,7,10-tetraacetic acid).[20] In the presence of Ca^{2+} and Zn^{2+} ions, the formation of hydroxo complexes was observed at high pH values (Fig. 9 and Fig. 10). As expected, the hexadentate $Me_2DO2PME$ ligand gave more stable complexes with Cu^{2+} and Zn^{2+} rather than with Ca^{2+} and Gd^{3+}.

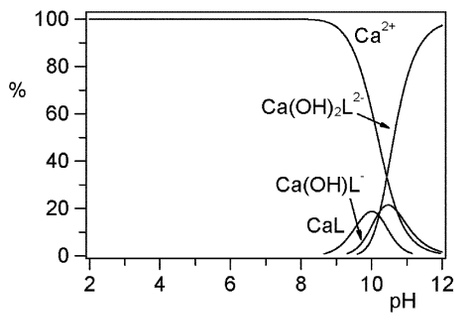

Fig. 9 Speciation diagram for the system Ca^{2+}–$Me_2DO2PME$ system (298 K, $I = 0.1$ mol dm^{-3} NMe_4Cl, metal to ligand ratio 1:1, $C_M = 0.001$ mol dm^{-3}). Species percentages are relative to total metal.

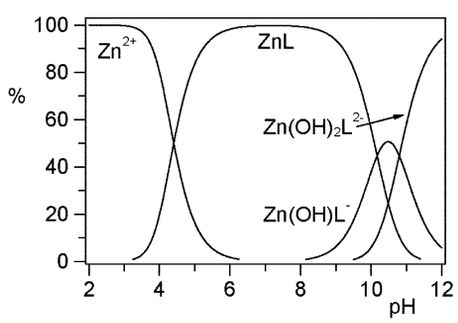

Fig. 10 Speciation diagram for the system Zn^{2+}– $Me_2DO2PME$ system (298 K, $I = 0.1$ mol dm^{-3} NMe_4Cl, metal to ligand ratio 1:1, $C_M = 0.001$ mol dm^{-3}). Species percentages are relative to total metal.

The low stability of the Gd^{3+} complex is a likely consequence of the strong effect of both the nature and number of pendant monoethyl ester phosphonate groups. The stability constant indicates that $Me_2DO2PME$ forms a significantly less stable complex with Gd^{3+} (about 10 order of magnitude) than the carboxylate macrocycle DO2A,[21] consistent with the weakly basic $P(O)(OEt)O^-$ groups.

Concluding remarks

A new hexadentate macrocycle ligand, $Me_2DO2PME$, containing two monoethyl ester phosphonate acid arms has been synthesized and employed to bind copper(II) ions. The resulting neutral complex $[Cu(Me_2DO2PME)]$ is octahedrally coordinated by the four nitrogen atoms of the macrocycle and two oxygen atoms from the phosphonate groups. This complex shows a remarkable thermodynamic stability in the pH range from 2.5 to 7 where neither protonated nor hydroxylated species are formed. Excellent stability is also shown by complexes of $Me_2DO2PME$ with Zn^{2+}.

The coordination behaviour of $Me_2DO2PME$ forecasts the formation of lanthanide complexes containing at least two water molecules in the inner coordinating sphere to complete the coordination of metal centres. By doing so, the water proton relaxivity of such complexes should increase, as reported

by Sherry and co-workers for GdDO2A$^+$ (DO2A = 1,4,7,10-tetraazacyclododecane-1,7-diacetic acid).[20]

Experimental

General information

Deuterated solvents for NMR measurements (Merck, Aldrich) were dried over molecular sieves. Analytical grade NMe_4Cl (Merck) was purified by double recrystallization from ethanol–water mixtures before use. 4,10-Dimethyl-1,4,7,10-tetraazacyclododecane was prepared as described in literature.[22] All the other reagents and chemicals were reagent-grade and used as received from commercial suppliers. Infrared spectra were recorded on a Perkin–Elmer 1600 Series FT-IR spectrophotometer using samples mulled in Nujol between KBr plates. UV/Visible spectra were recorded on a Perkin–Elmer Lambda 9 Spectrometer. Molar susceptibility analyses were performed on a Sherwood Scientific MSB AUTO balance. GC analyses were performed on a Shimadzu GC-14A gas chromatograph equipped with a flame ionization detector and a 30 m (0.25 mm id, 0.25μm film thickness) SPB-1 Supelco fused silica capillary column. GC/GM analyses were performed on a Shimadzu QP 5000 apparatus equipped with a column identical to that used for GC analyses. Elemental analyses (C,H,N) were performed using a Carlo Erba Model 1106 elemental analyzer.

Syntheses

4,10-Dimethyl-1,4,7,10-tetraazacyclododecane-1,7-bis(methanephosphonic acid diethyl ester)

4,10-Dimethyl-1,4,7,10-tetraazacyclododecane (3.46 g, 17.27 mmol) was dissolved in dry toluene (50 cm^3) containing dried/activated 4 Å molecular sieves and diethyl phosphite (4.89 cm^3, 38 mmol) added. The mixture was stirred under nitrogen and dry paraformaldehyde (1.29 g, 43.18 mmol) was added in small portions during 40 min. After heating for 2 h at 90 °C, the yellow solution was cooled to room temperature, filtered off and the filtrate was evaporated to dryness to give a viscous yellow oil (7.74 g, 90%). δ_H (300.11 MHz, $CDCl_3$, 25 °C, Me_4Si): 1,98 (12 H, t, $POCH_2CH_3$, $^3J_{HH}$ 7,2), 2.13 (6 H, s, NCH_3), 2.65 (8 H, br, $CH_3NCH_2CH_2$), 2.95 (8 H, br $CH_3NCH_2CH_2$), 2.98 (4 H, d, NCH_2P, $^2J_{HP}$ 9.30), 4.2 (8 H, pseudo quintet, $POCH_2CH_3$, $^3J_{HP}$ 7.2, $^3J_{HH}$ 7.2); δ_P(121.41, $CDCl_3$, 25 °C, H_3PO_4): 27.9 (s). δ_C(75.43 MHz, $CDCl_3$, pH 2.0, 25 °C): 17.62 (d, OCH_2CH_3, $^3J_{CP}$ 5.5), 44.60 (NCH_3), 52.73 (d, NCH_2P $^1J_{CP}$ 155), 54.66 ($CH_3NCH_2CH_2$), 56.93 ($CH_3NCH_2CH_2$) 62.74 (d, $POCH_2CH_3$, $^2J_{CP}$ 6.0 Hz). (Found: C, 52.90; H, 7.48; N, 6.90 %. $C_{20}H_{32}N_2P_2O_6$ requires C, 52.40; H, 7,04; N, 6.11%; *M*, 500.56).

4,10-Dimethyl-1,4,7,10-tetraazacyclododecan-1,7-bis(methanephosphonic acid monoethyl ester potassium salt) (Me_2DO2PME) (LK_2)

4,10-Dimethyl-1,4,7,10-tetraazacyclododecan-1,7-bis(methanephosphonic acid diethyl ester) (4.31 g, 8.6 mmol) was suspended in H_2O (20 cm^3), potassium hydroxide (3 M, 9.5 cm^3, 25.9 mmol) added and stirred while refluxing for 5 h. The mixture was then cooled to room temperature, filtered off and the solution was evaporated to dryness. The solid was dissolved in benzene (3 × 15 cm^3) and evaporated again. The residue was taken with methylene chloride (40 cm^3), dried over Na_2SO_4, and filtered. Removal of the solvent gave a pale yellow solid which was recrystallised from methylene chloride–diethyl ether (3:1 v/v) to yield a white microcrystalline, very hygroscopic, solid. (3 g, 77%)

The numbering scheme for the carbon and hydrogen atoms is given in Fig. 2.

δ_H (400.13 MHz, D_2O, pH 1, 25 °C, Me_4Si): δ 3.96 (4 H, pseudo quintet, H_E, $^3J_{HP}$ 7.02, $^3J_{FE}$ 7.04), 3.38 (4 H, ddd, H_B, $^2J_{BB'}$ 14.01, $^3J_{BC}$ 3.4, $^3J_{B\,C'}$), 3.18 (4 H, ddd, $H_{B'}$, $^3J_{B'C}$ 7.5, $^3J_{B'C'}$ 3.04), 3.03 (4 H, ddd, H_C, $^2J_{CC'}$ 15.4), 2.98 (6 H, s, H_A), 2.88 (4 H, ddd, $H_{C'}$), 2.80 (4 H, d, H_D, $^2J_{HP}$ 10.84), 1.15 (6 H, t, H_F, $^3J_{FE}$ 7.07 Hz); δ_C(100.61 MHz, D_2O, pH 1.0, 25 °C): 62.06 (C_E, d, $^2J_{CP}$ 6.0), 53.30 (C_B, s), 49.67 (C_C, d, $^3J_{PC}$ 7.0), 49,29 (C_D, d, $^2J_{CP}$ 157.95), 42.78 (C_A, s), 15.82 (C_F, d, $^3J_{PC}$ 5.01); δ_P(161.98 MHz, D_2O, pH, 1.0, 25 °C) 23.16 (s). (Found: C, 34.80; H, 7.84; N, 10.70%. $C_{16}H_{36}P_2N_4O_6K_2{\cdot}2H_2O$ requires C, 34.52; H, 7.24; N, 10.06%; *M*, 566.66).

Synthesis of [Cu(Me_2DO2PME)]·3H_2O (CuL)

CAUTION: Perchlorate salts of metal complexes are potentially explosive and must be handled with care. K_2Me_2DO2PME (0.4 g, 0.72 mmol) was dissolved in methanol (10 cm^3) and the pH was adjusted to 7.4 by addition of 3 M HCl. A solution of $Cu(ClO_4)_2{\cdot}6H_2O$ (0.72 mmol) in methanol (5 cm^3) was slowly added to the above solution at room temperature. White crystals of potassium perchlorate immediately separated which were filtered off and dibutyl ether (10 cm^3) was added to the blue solution. Partial evaporation of the solvent led to a blue oil which was taken up with diethyl ether, from which it solidified upon stirring. The very hygroscopic blue solid was filtered off, washed with diethyl ether and dried in a stream of nitrogen to constant weight.

Yield 80%. (Found: C, 34.6; H, 7.98; N, 10.21%. $C_{16}H_{42}N_4O_9P_2Cu{\cdot}3H_2O$ requires C, 34.42; H, 7.56; N, 10.00%; *M*, 560.02); IR ν/cm^{-1} 1610 (PO). $\lambda_{max}(H_2O)$/nm (ε_{max}/dm^3 mol^{-1} cm^{-1}) 591 (130), pH 7. μ_{eff} = 2.08 BM.

NMR measurements

^{1}H, ^{13}C{^{1}H} and ^{31}P{^{1}H} NMR spectra were recorded at 200.13, 50.32 and 81.01 MHz, respectively, on a Bruker 200-ACP spectrometer or at 400.13, 125.76 and 161.8 MHz, respectively, on a Bruker Avance DRX-400 spectrometer. Chemical shifts are relative to tetramethylsilane as external reference or were calibrated against solvent resonances. The assignments of the signals resulted from 2D–^{1}H COSY and proton detected ^{1}H–^{13}C correlations using degassed non-spinning samples. 2D NMR spectra were recorded on a Bruker Avance DRX-400 spectrometer using pulse sequences suitable for phase-sensitive representations using TPPI (time proportional phase incrementation). The ^{1}H–^{13}C correlations[23] were recorded using an HMQC (heteronuclear multiple quantum correlation sequence) sequence which allows for the measurements of J_{HC} coupling constants. Solutions of Me_2DO2PME (0.03 M) for NMR pH titration were prepared in D_2O and the desiderated pD was adjusted with standard 1 M solutions of DCl or KOD. The final pD was determined with an Orion Research 601 I Digital Ionalyzer apparatus equipped with combined glass Ag/AgCl microelectrode (Ingold) which was standardized against standard aqueous buffers at pH 4 and 7. The final pD was calculated using the empirical relationship pD = pH + 0.40.[24] The ^{1}H, ^{31}P and ^{13}C NMR spectra for pH titrations were performed on the Bruker ACP200 (200.13; 50.32 MHz) instrument at a probe temperature of 25 °C. ^{31}P shifts were referenced to external 85% H_3PO_4 with downfield values taken as positive.

Potentiometry

All pH-metric (pH = −log [H$^+$]) measurements employed for the determination of protonation and complex formation constants were carried out in 0.10 mol dm^{-3} NMe_4Cl solutions at 298.2 ± 0.1 K, by using the equipment and the methodology that has been previously described.[13] The combined Metrohom glass electrode was calibrated as a hydrogen concentration probe by titrating known amounts of HCl with CO_2-free

NMe_4OH solutions and determining the equivalence point by Gran's method[25] which allows one to determine the standard potential $E°$ and the ionic product of water ($pK_w = 13.83 \pm 0.1$ at 298.2 ± 0.1 K in 0.15 mol dm^{-3} NMe_4Cl). Carbon dioxide-free water was produced from deionised water which was twice distilled in a quartz apparatus and stored under purified nitrogen. An approximately 0.10 mol dm^{-3} $[Me_4N]OH$ solution, prepared by dilution of commercial concentrated solution (Fluka), was stored under nitrogen and its concentration was checked before and after each potentiometric experiment by titration against potassium hydrogen phthalate (Fluka). A 0.1 mol dm^{-3} stock solution of copper chloride was prepared by dissolving analytical grade $CuCl_2 \cdot 2H_2O$ (Merck) in water and the copper(II) content was determined gravimetrically as its salycylaldoximate complex.[26]

At least three measurements (about 30 data points each one) were performed for each system in the pH ranges 2.0–12 for ligand protonation and 2.5–10.5 for complexation experiments. The total ligand concentration was about 7×10^{-4} mol dm^{-3} in all measurements while the metal ion concentration in the complexation experiments was in the range 2×10^{-4}–9×10^{-4} mol dm^{-3} for Ca^{2+}, $Cu^{2+}$and Zn^{2+}. 97 data points from three curves were used for the determination of the protonation constants; 122, 113 and 133 data points were used for the determination of complex formation constants for Ca^{2+}, $Cu^{2+}$and Zn^{2+}, respectively. Steady emf readings after the addition of each aliquot of the hydroxide solution were attained fairly rapidly in the protonation and in the Ca^{2+} and Zn^{2+}experiments, whereas in the Cu^{2+} complex formation measurements it was inevitable to wait up to 30 minutes in the pH region above pH 5 and it was necessary to stop the titration at pH > 7, because the equilibrium was not reached after more than one hour. Complexation reactions of Gd^{3+} with $Me_2DO2PME$ are slow; about four weeks are necessary to achieve the final equilibrium. For this reason out-of-cell experiments were performed in which 10 individual solutions, in the approximate pH range 2.5–6, corresponding to single points of a conventional titration were stored in a thermostat at 298.2 ± 0.1 K, and their pH was periodically controlled to ensure the achievement of equilibrium conditions. The corresponding emf data were used to determine the equilibrium constants of the complex species. In the complexation experiments ligands and metal ion concentrations were 1×10^{-3} mol dm^{-3}. The computer program HYPERQUAD was used to calculate the equilibrium constants from emf data.[27]

X-band EPR spectra

The X-band EPR spectra were recorded on the BRUKER Spectrometer ER 200-SR D operating at $\nu = 9.44$ GHz. The H*0* applied magnetic field was calibrated by using a Varian F-8 Fluxmeter and the operational frequency ν was tested with a Hewlett-Packard X5-32B Wavemeter by using the solid state sample DPPH (diphenylpicrylhydrazyl free radical) as suitable field marker ($g_{averaged}$ (DPPH) = 2.0036(5)). The actual temperature was controlled with a Bruker B-ST 100/70 unit (T accuracy = ±1K). The a_i hyperfine coupling splittings were measured by the peak-to-peak distances of the four cupric isotropic or anisotropic lines in the corresponding signals, and the relevant A_i hyperfine coupling constants calculated.[17] The best fit computed values of the cupric parameters were evaluated by using appropriate simulation procedures.[18] To have quantitative reproducibility the cupric samples were introduced into a calibrated quartz capillary tube permanently positioned in the resonance cavity. The copper(II) complex samples were prepared by dissolving weighed amounts of CuL complex in MeOH, CH_2Cl_2 and H_2O solvents with millimolar concentrations, in order to ensure high spectral resolution (cupric water solutions are poorly resolved, particularly at liquid nitrogen conditions (T = 100 K)).

Cyclic voltammetry

The apparatus for electrochemistry has been described elsewhere.[28] Cyclic voltammetry and controlled potential coulometry have been performed in (anhydrous) DMSO (Aldrich) solution containing $[NBu_4][ClO_4]$ (electrochemical grade, Fluka) (0.1 mol dm^{-3}) as supporting electrolyte. All the potential values are referred to the saturated calomel electrode (SCE). Under the present experimental conditions the one-electron oxidation of ferrocene occurs at $E°' = +0.38$ V, *vs.* SCE.

Acknowledgements

We thank the Consiglio Nazionale delle Ricerche (CNR) for financial support (CNR-Agenzia 2000 CNR00AAF-002). Thanks are due to Dr Pierluigi Barbaro (ICCOM-CNR) for carrying out 2D-NMR spectra and to Dr Maurizio Peruzzini (ICCOM-CNR) for helpful discussion.

References

1 (*a*) S. F. Lincoln, *Coord. Chem. Rev.*, 1977, **166**, 255–272; (*b*) L. F. Lindoy, *Adv. Inorg. Chem.*, 1997, **45**, 75–125; (*c*) K. P. Wainwright, *Coord. Chem. Rev.*, 1997, **166**, 35–45; (*d*) M. Meyer, V. Dahaoui-Gindrey, C. Lecomte and R. Guillard, *Coord. Chem. Rev.*, 1978, **178**, 1313–1328.
2 C. J. Anderson, J. M. Connett, S. W. Schwarz, P. A. Rocque, L. W. Guo, G. W. Philpott, K. R. Zinn, C. F. Meares and M. J. Welk, *J. Nucl Med.*, 1992, **33**, 1685–1691.
3 B. E. Rogers, C. J. Anderson, J. M. Connett, L. W. Guo, W. B. Edwards and E. L. C. Sherman, *Bioconjugate Chem.*, 1996, **7**, 511–526.
4 P. M. Smith-Jones, R. Fridich, T. A. Kaden, I. Novak-Hofer, K. Siebold, D. Tschudin and H. R. Maecke, *Bioconjugate Chem.*, 1991, **2**, 415–422.
5 (*a*) D. Parker, in *Comprensive Supramolecular Chemistry*, Ed. J. M. Lehn, Pergamon, Oxford, 1996, vol. 10, p. 487; (*b*) S. Aime, M. Botta, M. Fasano and E. Terreno, *Acc. Chem. Res*, 1999, **99**, 951–966; (*c*) P. Caravan, J. J. Ellison, T. J. Mc Murry and R. B. Laufer, *Chem Rev.*, 1999, **99**, 2293–2312.
6 W. A. Volker and T. J. Hoffmann, *Chem. Rev.*, 1999, **99**, 2269–2278; V. Alexander, *Chem. Rev.*, 1995, **95**, 273–183; D. Parker, *Chem. Soc. Rev.*, 1990, **19**, 271–283; D. Parker and K. J. Jankowski, in *Advances in Metals in Medicine*, eds. M. J. Abrams and B. A. Murrer, Jai Press, New York, 1993, vol. 1, ch. 2, p. 29; K. Devreese, V. Kofler-Mongold, C. Leutgeb, V. Weber, K. Vermeire, S. Schacht, J. Anne, E. De Clercq, R. Datema and G. Werner, *J. Virol.*, 1996, **70**, 689–696.
7 C. J. Anderson and M. J. Welch, *Chem. Rev.*, 1999, **99**, 2219–2233; S. Liu and D. S. Edwards, *Chem. Rev.*, 1999, **99**, 2235–2243; E. Soini, L. Hemmila and P. Dhalen, *Ann. Biol. Clin. (Paris)*, 1990, **48**, 567–575; R. A. Evangalista, A. Pollak, B. Allore, E. F. Templeton, R. C. Morton and E. P. Diamandis, *Clin. Biochem.*, 1988, **21**, 173–189; E. Lopez, C. Chypre, B. Alpha and G. Mathis, *Clin. Chem.*, 1993, **39**, 196–204; G. Mathis, *Clin. Chem.*, 1995, **41**, 1391–1404; E. Soini and H. Kojola, *Clin. Chem.*, 1983, **29**, 65–76; I. Hemmila, V. M. Mukkala and S. Dakubu, *Anal. Biochem.*, 1984, **137**, 375–384.
8 E. F. G. Dickson, A. Pollak and E. P. Diamandis, *Photochem. Photobiol.*, 1995, **27**, 3; A. D. Sherry, *J. Less-Common. Met.*, 1989, **149**, 133–143.
9 R. Hancock, in *Perspectives in Coordination Chemistry*, eds. A. F. Williams, C. Floriani and A. E. Nurbach, *Verlag Helv. Chim. Acta*, Basel, 1992, p. 129.
10 (*a*) A. D. Sherry, *J. Alloys Comp*, 1997, **249**, 153; (*b*) F. I. Belskii, Y. M. Polikarpov and M. I. Kabachnik, *Usp. Khim*, 1992, **61**, 415–422.
11 (*a*) E. Cole, R. C. Copley, J. A. K. Howard, D. Parker, G. Ferguson, J. F. Gallagher, B. Kaitner, A. Harrison and L. Royle, *J. Chem. Soc., Dalton Trans.*, 1994, 1619; (*b*) D. Parker, in *Comprehensive Supramolecular Chemistry*, eds. J. L. Atwood, D. D. MacNicol, J. E. D. Davies, F. Vogtle, J. M. Lehn, D. N. Reinhoudt, Pergamon, Oxford, 1996, vol. 10, ch. 17; (*c*) A. Harrison, C. A. Walker, K. A. Pereira, D. Parker, L. Royle, K. Pulukkody and T. J. Norman, *Mag. Reson. Imaging.*, 1993, **11**, 701–712.
12 T. J. Norman, D. Parker, L. Royle, A. Harrison, P. Antoniw and D. J. King, *J. Chem. Soc., Chem. Commun.*, 1995, 1877–1978.

13 P. Barbaro, C. Bianchini, G. Capannesi, L. Di Luca, F. Laschi, D. Petroni, P. A. Salvadori, A. Vacca and F. Vizza, *J. Chem. Soc., Dalton Trans.*, 2000, 2393–2401.
14 L. Burai, J. Ren, Z. Kovacs, E. Bruker and A. D. Sherry, *Inorg. Chem.*, 1998, **37**, 63–75.
15 C. F. G. C. Geraldes, A. D. Sherry and W. P. Cacheris, *Inorg. Chem.*, 1989, **28**, 3336–3341.
16 I. Lukes, P. Hermann and P. Pech, *Collect. Czech. Chem. Commun.*, 1989, **28**, 653–672.
17 (*a*) J. R. Pilbrow, in *Transition Ion Electron Paramagnetic Resonance*, Clarendon Press, Oxford 1990; (*b*) F. E. Mabbs and D. Collins, in *Electronic Paramagnetic Resonance of d transition Metal Compounds*, Elsevier, Amsterdam 1992.
18 (*a*) J. P. Lozos, B. M. Hofman and C. G. Franz, *QCPE*, 1974, **20**, 295; (*b*) G. Della Lunga, *ESRMGR Simulation Program*, Department of Chemistry, Siena, 1994.
19 J. Peisach and W. E. Blumberg, *Arch. Biochem. Biophys.*, 1974, **175**, 691–712.
20 J. Huskens, Z. Kovacs, J. P. Andrè, C. F. G. C. Geraldes and A. D. Sherry, *Inorg. Chem.*, 1997, **36**, 1495–1503.
21 A. Bianchi, L. Calabi, F. Corana, S. Fontana, P. Losi, A. Maiocchi, L. Paleari and B. Valtancoli, *Coord. Chem. Rev.*, 2000, **204**, 309–3993.
22 M. Ciampolini, M. Micheloni, N. Nardi, P. Paoletti, P. Dapporto and F. Zanobini, *J. Chem. Soc., Dalton Trans.*, 1984, 1357–1362.
23 M. F. Summers, L. G. Marzilli and A. Bax, *J. Am. Chem. Soc.*, 1986, **108**, 4285–4294.
24 (*a*) P. K. Glasoe and F. A. Long, *J. Phys. Chem.*, 1960, **64**, 188–193; (*b*) K. Mikkelsen and S. O. Nielsen, *ibid.*, 1960, **64**, 632; (*c*) R. G. Bates, *Determination of pH. Theory and Practice*, Wiley, New York, 2nd edn, 1973, pp. 252–253 and 375–376; (*d*) R. Delgado, J. J. Frausto. Da Silva, M. T. S. Amorim, M. F. Cabral, S. Chaves and S. Costa, *Anal. Chim. Acta*, 1991, **245**, 271–278.
25 G. Gran, *Analyst*, 1952, **77**, 661–669.
26 I. M. Kolthoff and E. B. Sandell, in *Textbook of quantitative inorganic analysis*, eds. The MacMillan Company, New York, 1967.
27 P. Gans, A. Sabatini and A. Vacca, *Talanta*, 1986, **43**, 1739–1753.
28 A. Togni, M. Hobi, G. Rihs, G. Rist, A. Albinati, P. Zanello, D. Zech and H. Keller, *Organometallics*, 1994, **13**, 1224–1234.